

Assignment of the relative stereochemistry of the spiroptides, macrocyclic toxins isolated from shellfish and from the cultured dinoflagellate *Alexandrium ostenfeldii*

Michael Falk, Ian W. Burton, Tingmo Hu,[†] John A. Walter* and Jeffrey L. C. Wright[‡]

Institute for Marine Biosciences, National Research Council of Canada, 1411 Oxford Street, Halifax, NS, Canada B3H 3Z1

Received 20 July 2001; revised 20 August 2001; accepted 21 August 2001

Abstract—The relative stereochemistry of 13-desmethyl spiroptide C, except for one chiral center, has been determined from NMR data by means of ConGen, a molecular modeling method which applies high-temperature molecular dynamics under distance constraints generated from NOESY and ROESY data. The method shows this spiroptide to have the same relative stereochemistry as pinnatoxins A and D in the region of their common structure. Applicability of the ConGen method to molecules of this type is further justified by demonstrating that it yields the correct relative stereochemistry of the pinnatoxins when used with constraints generated from published data. The relative stereochemistries of spiroptides B and D are also determined by comparisons of their NMR data with 13-desmethyl spiroptide C and further application of ConGen. Crown Copyright © 2001 Published by Elsevier Science Ltd. All rights reserved.

1. Introduction

Spiroptides A–D (**1–4**) and 13-desmethyl C (**5**) are macrocyclic compounds,^{1–3} that are toxic in the mouse bioassay for lipophilic toxins.⁴ They were first found in extracts of shellfish from aquaculture sites that had been exposed to marine algal blooms. Structural features without stereochemistry were previously determined for the compounds from NMR and mass spectrometric data,^{1–3} and subsequently it was shown⁵ that they are produced by dinoflagellates such as *Alexandrium ostenfeldii*. The compounds **1–5** (Fig. 1) all contain an unusual cyclic imine moiety with the same atomic connectivity as that found in the pinnatoxins^{6–9} and pteriatoxins,¹⁰ and resembling parts of gymnodimines A and B^{11–13} which are also toxic in the mouse bioassay. The intact cyclic imine ring is essential for toxicity, as the keto amine spiroptide derivatives E and F, in which this ring has been opened, are inactive in the mouse bioassay.²

The stereochemistry of the spiroptides is of interest for future toxicological studies, and also because the compounds are known to originate in dinoflagellates. Stereochemical similarity between the spiroptides and the pinnatoxins, for which the ultimate origin is unknown, would be further evidence to

suggest a dinoflagellate source for the latter. Over several years, small quantities of spiroptides have been isolated from shellfish tissue and plankton biomass, and more recently from laboratory cultures of *A. ostenfeldii*, but crystals have not been obtained.

The amount of stereochemical detail revealed by NOE and coupling data from ¹H NMR is highly dependent on the degree of structural flexibility and on the number and distribution of protons. In larger molecules, it becomes increasingly difficult to correlate stereochemistry among different moieties to obtain total configuration, and to be confident that any proposed overall structure is the only one consistent with the data. Many shellfish toxins, including the spiroptides, pose such structural problems and the use of molecular modeling to relate NOE data and stereochemistry in molecules with known atomic connectivity is indicated.

The work reported here establishes the relative stereochemistry of 13-desmethyl spiroptide C (**5**) directly from NMR data by means of molecular modeling, and that of spiroptides B (**2**) and D (**4**), for which the NMR data are more ambiguous, by modeling and comparison with **5**. Using Tripos Sybyl molecular modeling software we previously developed a routine (ConGen[¶]) for this purpose in Sybyl Programming Language.¹⁴ More recently, we

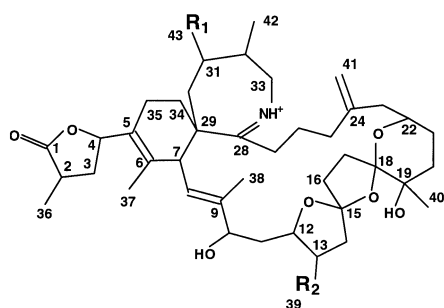
Keywords: spiroptide; stereochemistry; phycotoxin; pinnatoxin; NMR; molecular modeling; ConGen.

* Corresponding author. Tel.: +1-902-426-6458; fax: +1-902-426-9413; e-mail: john.walter@nrc.ca

[†] Present address: Andrx Corporation, Fort Lauderdale, FL 33314-4030, USA.

[‡] Present address: UNC Wilmington Center for Marine Sciences, 1 Marvin Moss Lane, Wilmington, NC 28409, USA.

[¶] Our ConGen routine should not be confused with other procedures called CONGEN (Yamdagni, N. *Nucl. Sci. Abstr.* **1971**, 25, 18777; Nourse, J. G.; Smith, D. H.; Carhart, R. E.; Djerassi, C. *J. Chem. Soc.* **1980**, 102, 6289–6295; Broccoleri, R. E.; Karplus, M. *Biopolymers*, **1987**, 26, 137–168).



Spirolide	R ₁	R ₂
1 A	Δ ^{2,3}	H
2 B		CH ₃
3 C	Δ ^{2,3}	CH ₃
4 D		CH ₃
5 13-desMe C	Δ ^{2,3}	H

Figure 1. Structures of spirolides A–D and desmethyl spirolide C.

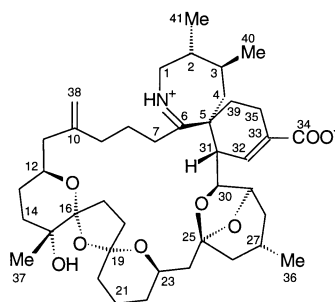
generated a similar routine (XMConGen) with HyperChem software for an SGI workstation. The latter routines differ from ConGen only in the types of constraints applied and in the force fields used (see Section 3). The validity of the ConGen approach has been assessed previously¹⁴ by applying it to compounds of known stereochemistry. In justification of its application to spirolides, we show in this report that the method will generate the known relative stereochemistry of pinnatoxins A (6) and D (7) (Fig. 2) from the published NOESY and ROESY data^{7,8} without recourse to scalar coupling data. We also demonstrate that the method is robust in that the stereochemical result does not require precise measurements of internuclear distances based on NOE. A similar approach based on distance geometry with random variation of chiral volume has been successfully used by others^{15–18} to determine relative stereochemistry of some natural products.

2. Results and discussion

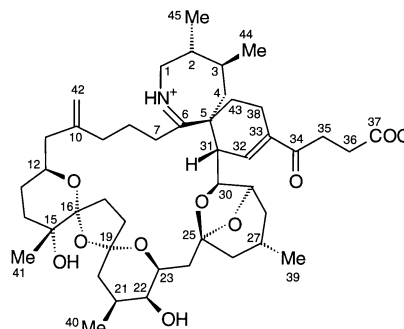
Assignments of NMR spectra of 2 and 4 in CD₃OD, and of 5 in CD₃OH, have been published.^{1–3} Table 1 shows previously unpublished assignments of 2 and 4 in CDCl₃, determined from 2D ¹H COSY, TOCSY and ¹H/¹³C HMQC and HMBC spectra. The 2D ¹H NOESY and ROESY

Table 1. ¹H and ¹³C resonance assignments for spirolides B 2 and D 4 in CDCl₃. Assignments deduced from ¹H COSY, TOCSY, NOESY and ROESY spectra, and from ¹H/¹³C HMQC and HMBC spectra. Temperature 20°C. Reference to C¹HCl₃=7.26 ppm (¹H); ¹³CHCl₃=77.0 ppm (¹³C)

C#	2 δ _C	2 δ _H	4 δ _C	4 δ _H
1	179.5		179.4	
2	35.8	2.70	35.7	2.70
3	35.3	1.66, 2.45	35.3	1.66, 2.45
4	77.7	5.26	77.7	5.27
5	127.7		127.9	
6	131.1		130.9	
7	47.6	3.49	48.1	3.49
8	122.4	5.29	122.3	5.13
9	141.7		141.8	
10	75.1	4.25	75.5	4.24
11	37.1	1.77, 2.02	36.6	1.72, 2.00
12	81.5	4.38	81.7	4.39
13	35.1	2.46	35.0	2.48
14	45.2	1.93, 2.24	45.3	1.94, 2.23
15	116.3		116.2	
16	35.4	2.04, 2.38	35.3	2.04, 2.38
17	30.8	1.81, 2.16	30.9	1.81, 2.15
18	111.1		111.0	
19	69.8		69.8	
20	35.8	1.65 (2)	35.8	1.61 (2)
21	29.0	1.25, 1.62	28.9	1.22, 1.58
22	68.3	3.96	68.2	3.95
23	46.1	2.03, 2.41	46.3	2.03, 2.41
24	147.1		147.0	
25	33.5	1.63, 2.08	33.7	1.67, 2.03
26	22.2	1.38, 2.08	22.1	1.36, 2.17
27	33.6	2.25 (2)	33.6	2.24 (2)
28	174.5		174.9	
29	49.8		49.1	
30	26.9	1.61, 1.83	37.5	1.54, 1.69
31	30.7	1.08, 1.77	35.7	1.16
32	32.2	1.90	39.9	1.36
33	52.5	3.59, 3.71	52.7	3.57, 3.74
34	31.4	1.60, 1.91	31.7	1.50, 1.92
35	20.0	1.90, 2.32	19.9	1.90, 2.33
36	15.0	1.30	15.0	1.30
37	16.5	1.54	16.5	1.54
38	13.8	1.88	14.1	1.90
39	15.1	1.18	15.1	1.18
40	20.9	1.23	21.0	1.22
41	110.0	4.73, 4.75	110.0	4.74, 4.76
42	20.4	0.92	18.7	0.99
43			21.1	0.94



6 Pinnatoxin A



7 Pinnatoxin D

Figure 2. Stereochemistry of pinnatoxins A (6) and D (7) from Refs. 7,8, inverted in accordance with absolute stereochemistry established in Ref. 20.

of the peaks on a four-level scale from strong (s) to very weak (vw) (see Section 3). Ambiguous cross-peaks are also shown in cases where another cross peak for the same proton pair is unambiguous in at least one of the datasets for **2**, **4** and **5**.

As **5** was available in larger amounts than the other spiro- lides and had a different distribution of ^1H chemical shifts, a larger number of unambiguous cross-peaks could be determined than for **2** and **4**. A series of NOESY and ROESY spectra were obtained for **5** over a range of mixing times under otherwise identical conditions of acquisition and data processing (see Section 3). Volume integrals of all peaks in the spectra yielded build-up curves for each resolved cross-peak, the initial build-up rates leading to ‘measured’ internuclear distances.¹⁹ These data for **5** are shown in Table 2. Average measured distances for each range of the four-level scale were: 2.3 Å for s, 2.5 Å for m, 2.9 Å for w and 3.2 Å for vw, with S.D. ca. 0.3 Å for s and m; ca. 0.5 Å for w and vw.

Data derived from the NOESY and ROESY spectra were imported into the ConGen and/or XMConGen molecular modeling programs as constraint tables, each corresponding to the unambiguous constraints in one of the columns of Table S2. For **5** the modeling was done independently with constraint tables of four different types (see Section 3) using the information in Table 2: (i) with interproton distances measured from build-up rates; (ii) with distances assigned according to the correspondence $s \leq 2.7$ Å, $m \leq 3.0$ Å, $w \leq 3.3$ Å, $vw \leq 3.6$ Å, where allowance is made for cross-peak variation with internuclear distance but the constraints approximate the upper bound, rather than the average, of the measured distribution corresponding to each strength range; (iii) with all constraint distances ≤ 2.7 Å, (iv) with all constraint distances ≤ 3.3 Å. Approaches (iii) or (iv) can be used when a cross peak is present, but no attempt is made to measure its strength or to estimate an internuclear distance. With **2** and **4**, approach (ii) was applied to spectra at 400 ms mixing time, as no build-up data were obtained. Approach (iii) was also used with pinnatoxins A (**6**) and D (**7**)^{7,8} to transcribe observed NOE connectivities of unspecified strength into a constraint table for testing of ConGen with published data (see below).

The ConGen¹⁴ and XMConGen methods compare a set of interproton distances in a constraint table with a set generated in a molecular model subjected to constrained high temperature molecular dynamics, simulated annealing and energy minimization with the constraints removed. This process is repeated for many cycles, where scoring criteria for the structure produced by each cycle are used to determine whether the structure is consistent with the constraints. The goal is to generate a unique optimum configuration and its enantiomer. Where there is insufficient information, the approach should still generate a set of structures compatible with the available data. The results for each structure are obtained as a table of: (a) interproton distances d_i corresponding to the constraints; the chirality (*R* or *S*) in order of ascending carbon number; (b) the energy *E*; (c) the number *V* of violations of constraints by more than an arbitrary percentage, typically 10–20%; and (d) the RMS deviation σ in Å, where $\sigma^2 = (1/N) \sum (d_i - D_i)^2$

Table 2. Strengths of unambiguous ^1H - ^1H NOESY and ROESY cross peaks and measured interproton distances for proton pairs in 13-desmethyl spiro- lide **5** in CD_3OH

Proton A	Proton B	NOE strength	Measured distance (Å)
H3	H4	s	2.8
H3	H34b	w	3.6
H3a	H37	w	3.0
H4	H27b	vw	DU (3.6)
H4	H34b	vw	3.7
H4	H37	s	2.2
H7	H27a	w	2.4
H7	H27b	s	2.1
H7	H34b	m	2.6
H7	H37	m	DU (3.0)
H7	H38	s	2.3
H8	H10	s	2.6
H8	H11b	w	2.9
H8	H27b	w	DU (3.3)
H8	H30b	m	2.4
H8	H31	m	2.5
H8	H37	w	DU (3.3)
H8	H43	m	2.9
H10	H11b	m	2.6
H10	H12	w	3.6
H10	H13a	m	2.5
H10	H43	vw	2.8
H11b	H13b	m	2.4
H11b	H22	m	2.7
H11b	H27b	vw	DU (3.6)
H12	H13a	s	2.2
H12	H14a	s	DU (2.7)
H12	H14b	m	3.0
H17a	H40	m	2.6
H17b	H40	w	2.7
H20a	H22	m	2.2
H20a	H42	vw	DU (3.6)
H20b	H40	m	2.4
H21a	H41b	vw	DU (3.6)
H21b	H40	w	DU (3.3)
H22	H23a	m	2.4
H22	H40	vw	DU (3.6)
H26a	H41b	w	2.5
H27a	H34b	w	2.8
H27b	H38	s	2.5
H30a	H43	vw	3.0
H30b	H43	m	2.3
H32	H33a	w	2.4
H32	H33b	w	DU (3.3)
H32	H42	m	DU (3.0)
H32	H43	m	2.4
H33a	H34a	s	2.0
H33a	H42	w	DU (3.0)
H33b	H42	m	2.5

Strength designations (see Section 3) are: s=strong, m=medium, w=weak, vw=very weak. Interproton distances for **5** determined from NOESY and ROESY build-up rates (see text, error ca. ± 0.3 Å for corresponding strengths s or m; ca. ± 0.5 Å for w or vw), DU=distance undetermined, assigned distance in brackets.

for $d_i > D_i$. Here, d_i is an interproton distance and D_i is the constraint distance, below which the constraining force becomes zero. A successful structure is one that, over a series of cycles (typically 500–1000), occurs with high frequency along with its enantiomer, and has a low σ , a low *V*, as well as a low *E*. In previous tests¹⁴ a correct optimum structure was usually returned if the number of constraints was greater than ca. 2–3 times the number of chiral centres, and results were relatively insensitive to inaccuracies in the constraining interproton distances.

Table 3. Stereochemistry of pinnatoxin A and D as reported by earlier authors and as determined by ConGen

Position	C2	C3	C5	C12	C15	C16	C19	C21	C22	C23	C25	C27	C28	C29	C30	C31
Pinnatoxin A (6)																
Published structure																
Ref. 7 ^a	<i>R</i>	<i>S</i>	<i>R</i>	<i>S</i>	<i>R</i>	?	<i>R</i>	ach	ach	<i>R</i>	<i>R</i>	<i>R</i>	<i>R</i>	<i>R</i>	<i>S</i>	<i>S</i>
Ref. 7 ^b	<i>R</i>	<i>S</i>	<i>R</i>	<i>S</i>	?	<i>R</i>	<i>R</i>	ach	ach	<i>R</i>	<i>R</i>	<i>R</i>	<i>R</i>	?	?	?
Ref. 17 ^c	<i>R</i>	<i>S</i>	<i>R</i>	<i>S</i>	<i>R</i>	<i>R</i>	<i>R</i>	ach	ach	<i>R</i>	<i>R</i>	<i>R</i>	<i>R</i>	<i>R</i>	<i>S</i>	<i>S</i>
ConGen	<i>R</i>	<i>S</i>	<i>R</i>	<i>S</i>	<i>R</i>	<i>R</i>	<i>R</i>	ach	ach	<i>R</i>	<i>R</i>	<i>R</i>	<i>R</i>	<i>R</i>	<i>S</i>	<i>S</i>
Pinnatoxin D (7)																
Published structure																
Ref. 8 ^d	<i>R</i>	<i>S</i>	<i>R</i>	<i>S</i>	<i>R</i>	?	?	<i>S</i>	<i>S</i>	<u><i>S</i></u>	<u><i>S</i></u>	<u><i>S</i></u>	ach	<i>R</i>	<i>S</i>	<i>S</i>
Ref. 8 ^e	<i>R</i>	<i>S</i>	<i>R</i>	<i>S</i>	?	<i>R</i>	<u><i>S</i></u>	?	?	<u><i>S</i></u>	<u><i>S</i></u>	<u><i>S</i></u>	ach	?	<i>S</i>	?
ConGen	<i>R</i>	<i>S</i>	<i>R</i>	<i>S</i>	<i>R</i>	<i>R</i>	<u><i>S</i></u>	(<i>S</i>)	(<i>S</i>)	(<u><i>S</i></u>)	(<u><i>S</i></u>)	(<u><i>S</i></u>)	ach	<i>R</i>	<i>S</i>	<i>S</i>

Underlining (*R*, *S*) indicates chirality in **7** trivially reversed with respect to **6** owing to priority changes. ach indicates a position that is achiral in this molecule. Question mark (?) indicates chirality ambiguous in this diagram. Parentheses (*S*) indicate some uncertainty in chirality determined by ConGen.

^a Chou et al.,⁷ Diagram 1 (reversed).

^b Chou et al.,⁷ Fig. 4 (reversed).

^c McCauley et al.,¹⁷ Diagram 1 (reversed).

^d Chou et al.,⁸ Diagram 1 (reversed).

^e Chou et al.,⁸ Fig. 2 (reversed).

2.1. Tests of ConGen with published data for pinnatoxins A and D

Constraint tables of type (iii) as described above were compiled from all NOE correlations denoted on structural diagrams or mentioned in the text of the publications describing the relative stereochemistry of pinnatoxins A (**6**)⁷ and D (**7**).⁸ The internuclear distance limits over which NOEs could be detected were not reported in these publications. Our use of 2.7 Å as a constraint distance implies that the forces applied in the molecular modeling are appropriate to ‘strong’ constraints in a type (ii) table. The total number of constraints available was 30 and 38 for pinnatoxin A and D, respectively. Despite the fact that the data were reported only as the presence or absence of an NOE without a corresponding strength estimate, and despite differences between the constraint tables for the two pinnatoxin structures, ConGen yielded the correct relative stereochemistry of both **6** and **7** (Table 3) without recourse to coupling-constant data.

In the case of **6**, the stereochemistry of all 14 chiral carbon atoms was determined with high certainty, the optimum structure *RSR SRR RRR RRR SS* (specified as chirality in order of increasing carbon number), and its enantiomer, occurring with much higher relative incidence (typically 43 vs 3 out of 969 ConGen cycles) and lower σ (typically 0.28 vs 0.36 Å) and slightly lower *V* (typically 6 vs 7) than the ‘second best’ structure. For **7**, the optimum structure *RSR SRR SSS SSS RSS* (and its enantiomer) occurred with higher relative incidence (typically 61 vs 17 out of 2311 ConGen cycles) but only very slightly lower σ (typically 0.28 vs 0.29 Å) and *V* (typically 6 vs 7) than the ‘second best’ structure *RSR SRR SRR RSS RSS* (and its enantiomer), which differed from the optimum structure by reversed chirality at C21, C22, and C23. Thus the relative stereochemistry of **7** was determined with certainty for only 12 out of its 15 chiral carbons, and with much lower certainty for the remaining three carbons. Comparison with the published relative stereochemistry of both **6**⁷ and **7**⁸ (Table 3) shows a perfect match in both cases, including carbons C21, C22, and C23 of **7**. The chiralities reported in Table 3 are for the enantiomer corresponding to the *absolute* structure of pinnatoxin A deduced by total synthesis by McCauley et al.,²⁰ which is now known to be the reverse of those shown in the diagrams in Refs. 7,8,20.

2.2. Stereochemistry of 13-desmethyl spirolide C found with ConGen

To help resolve ambiguities in the constraint table for **5**, spectra were recorded from two different preparations of the compound and at two temperatures (20 and –20°C). Corresponding peaks in **5** and other spirolides were cross-compared. Ultimately a list of 47 unambiguous constraints was drawn up (Table 2). Wherever possible, approximate internuclear distances were derived from initial build-up rates of NOESY and ROESY cross peaks (see Section 3). Previous testing¹⁴ indicated that this number of constraints should be sufficient to yield a unique configuration. Some very weak cross peaks which did not appear in all spectra, and for which distance estimates were not obtainable from

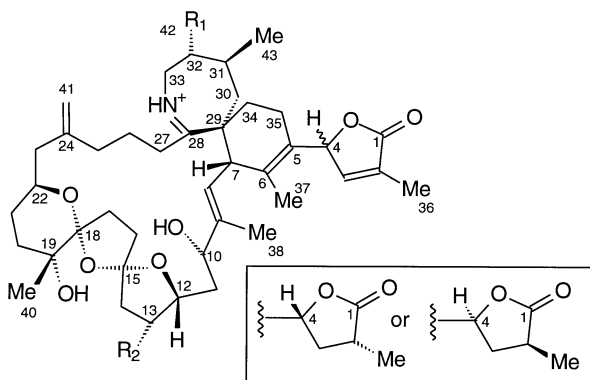


Figure 3. Relative stereochemistry of desmethyl spirolide C (**5**, R₁=CH₃, R₂=H) as determined from ConGen. Stereochemistry at C13 in spirolide B (**2**, R₁=H, R₂=CH₃) and in spirolide D (**4**, R₁=CH₃, R₂=CH₃) is also shown. The structure is presented in the same orientation as for pinnatoxins. Inset shows stereochemistry within lactone ring of **2** and **4**. The stereochemical relationship of this ring to the rest of the structure has not been determined.

build up rates, appeared to be impossible to satisfy with structures having low E , V and σ , and were not included in the final constraint table.

Both ConGen and XMConGen produced the same optimum configuration as indicated by minimum σ , despite differences in detailed approach due to the use of constraint lists of type (i), (ii), (iii) or (iv) and in the method of application of the constraints within each program (see above). The optimum configuration, specified as the chirality respectively at positions 4, 7, 10, 12, 15, 18, 19, 22, 29, 31 and 32, was (*S*)*SS SRR RSR SR*, shown in Fig. 3, or the enantiomer (*R*)*RR RSS SRS RS*. The brackets indicate an uncertainty in position 4. Indications of rotation of the C1–C4 lactone ring about the C4–C5 bond appeared in the form of close approaches that could not be satisfied simultaneously. These complicate the determination of chirality at C4, which remained undecided. In view of this uncertainty, the modeling was repeated with all constraints involving the lactone ring removed, resulting in the same optimum configuration for positions 7–32.

The lowest values of σ associated with best-fitting conformations of the optimum configuration were significantly smaller than for the second best stereomer, (*S*)*SS SRR RSR SS*. In a typical run of the ConGen program using all the 'measured distance' constraints in Table 2, the optimum stereomer occurred, with $\sigma \leq 0.47$ Å, 227 times out of 742 structures generated, the smallest σ being 0.39 Å. Of this total, the distribution over the four possible enantiomers (allowing for uncertainty at position 4) was 67:50:59:51, indicating complete and dense coverage of configuration space. The number of violations of constraints (by more than 10% of the constraining distance) was small ($V \geq 9$), and there were no large individual violations. The second best structure (*S*)*SS SRR RSR SS* occurred 7 times, with $\sigma = 0.41$ – 0.44 Å and $V \geq 11$, and the third best, (*S*)*SS RRR RSR SR*, 62 times with $\sigma = 0.44$ – 0.47 Å. As was found previously¹⁴, the resulting optimum configuration was not sensitive to the magnitude of distance constraints. A typical run using the measured distances in Table 2, but excluding the constraints to the lactone ring, resulted in an optimum configuration occurring with a higher relative incidence (typically 125 vs 22 out of 828 ConGen cycles), much lower σ (typically 0.23 vs 0.32 Å) and slightly lower V (typically 9 vs 11) than the second best structure, which was the same as above. Similar behaviour occurred with runs using XMConGen.

All H...H distances of the optimum configuration were examined and found to agree with the NOE data. All distances under 3.6 Å, short enough to expect an NOE signal, did in fact produce one, including those that were not used as constraints owing to ambiguity or overlap following from near-coincidence of two or more resonances.

Vicinal coupling constants $^3J_{\text{HH}}$ for **5** were measured from ¹H 1D spectra and 2D E.COSY spectra and examined for compatibility with the optimum structure and the next-best alternatives. The measurements were compared with calculated values based on average dihedral angles obtained from an ensemble of energetically minimized molecular models corresponding to each alternative stereochemical configuration. Calculations used the Haasnoot et al.²¹ empirical generalizations of the Karplus equation, specifically Eqs. (8) and (9) and Table 2 of that publication. Within the error of the measurements and calculations, there was no inconsistency with the stereochemistry (*S*)*SS SRR RSR SR* (and enantiomer). In particular, this stereomer predicts a dihedral angle H31–C31–C32–H32 ca. 163°, compatible with the large value (15.9 Hz) measured for $^3J(31,32)$ indicating an approximate *anti* conformation for this proton pair. The second best stereomer (*S*)*SS SRR RSR SS* generated from ConGen, which differed at position 32, predicts a dihedral angle ca. 38.5°, inconsistent with the large $^3J(31,32)$ observed.

2.3. Stereochemistry of spirolides B and D:

The available amounts of **2** and **4** were smaller than for **5**. NOESY and ROESY spectra were determined at a single mixing time in both methanol and chloroform, although the compounds were unstable in chloroform. Cross peaks were found to be generally comparable in all four datasets (**2** and **4**; methanol and chloroform), indicative of the same overall stereochemistry (Table S1 in supplementary data). ConGen was run independently on each of the four cases. It turned out that only partial stereochemistry could be determined, consistent in every case with that of **5** (Table 4). We note here the need for care in comparing *R* and *S* designations in these molecules owing to priority changes with different substitution patterns, as shown in Table 4.

2.4. Comparison with pinnatoxins

The ConGen approach based on NOEs alone is to be

Table 4. Stereochemistry of spirolides

Position	C2	C4	C7	C10	C12	C13	C15	C18	C19	C22	C29	C31	C32
DesMe spirolide C, from ConGen (5)	ach	nd	<i>S</i>	<i>S</i>	<i>S</i>	ach	<i>R</i>	<i>R</i>	<i>R</i>	<i>S</i>	<i>R</i>	<i>S</i>	<i>R</i>
Spirolides B and D, from ConGen and from comparison with data for 5 :													
B (2)	nd	nd	<i>S</i>	<i>S</i>	<u><i>R</i></u>	<i>R</i>	<u><i>S</i></u>	<i>R</i>	<i>R</i>	<i>S</i>	<u><i>S</i></u>	ach	<i>R</i>
D (4)	nd	nd	<i>S</i>	<i>S</i>	<u><i>R</i></u>	<i>R</i>	<u><i>S</i></u>	<i>R</i>	<i>R</i>	<i>S</i>	<u><i>R</i></u>	<i>S</i>	<i>R</i>
Pinnatoxin-A (in the region of spirolide-related structure)													
Position (6)							C16	C15	C12	C5	C3	C2	
							<i>R</i>	<i>R</i>	<i>S</i>	<i>R</i>	<i>S</i>	<i>R</i>	

nd indicates chirality could not be determined by ConGen. Underlining (*S*, *R*) indicates a trivial chirality reversal owing to priority changes. ach indicates a position that is achiral in this molecule. Chirality at C16 in **6** and at C18 in the spirolides was assumed to be *R*.

compared with the stereochemical elucidation of **6** and **7**.^{7,8} Those studies used primarily coupling data and also relied on non-quantitative NOE correlations to interrelate the different moieties. That procedure appears not to exclude the possibility that some alternate configuration might also be compatible with the data. The ConGen procedure, by producing a small set of stereoisomers compatible with the NOE data, following a constrained search over the total configuration space, reduces the risk that some compatible structures will be overlooked and simplifies the application of other data to resolve any remaining uncertainties.

The relative configuration of the spiroptides (Table 4) coincides with that of pinnatoxins A **6** and D **7** in the region of structural overlap. These marked structural similarities are further evidence for dinoflagellates as likely producing organisms for the pinnatoxins, as at least one dinoflagellate (*A. ostenfeldii*) is known to produce spiroptides.⁵

2.5. Deuterium exchange in spiroptides

In studies of spiroptides B and D using CD₃OD as a solvent, it was noted that H27a (the proton at C27 resonating at lower field) exchanges rapidly with deuterium from the solvent, whereas H27b is far more resistant to exchange. It is noteworthy that space-filling molecular models generated by ConGen, corresponding to the favoured stereochemistry above, show that H27a is highly exposed to the solvent while H27b is well protected by the remainder of the molecule.

3. Experimental

3.1. NMR Spectroscopy

Spectra of spiroptides B (**2**) and D (**4**) at 20°C in CD₃OD and CDCl₃ solution, and of 13-desmethyl spiroptide C (**5**) at 20 and –20°C in CD₃OH, were recorded at 11.7 T with Bruker AMX-500 and DRX-500 spectrometers. Standard Bruker pulse sequences were used for the respective classes of spectra, with solvent signal suppression by presaturation where appropriate. Assignments, including those previously published,^{1–3} were checked from 2D ¹H COSY, TOCSY and ¹H/¹³C HSQC or HMQC spectra, typically obtained with an acquisition time of ca. 0.11 s, 512*t*₁ increments, and a relaxation delay *D*₁ of 1–2 s. For **2** and **4**, 2D ¹H NOESY and ROESY spectra were recorded at mixing times of 300 and 400 ms. A more extensive dataset was generated with **5** in CD₃OH, for which mixing times of 50–1200 ms were used to provide NOESY and ROESY build-up data. E.COSY spectra of **5** were recorded with higher resolution (AQ 0.2 s, 1024*t*₁ increments). Spectra were processed with zero-filling in both dimensions.

Where cross peaks of NOESY and ROESY spectra were well resolved, internuclear distances (of type (i) above) for **5** were estimated from initial build-up rates of cross peak volumes by method (b) of Sykes and co-workers.¹⁹ Signals from geminal proton pairs separated by 1.8 Å were used for distance calibration. A list of such distance

estimates for unambiguously identified pairs of protons (Table 2) was used as one input for the modeling.

Simpler approaches (type (ii)–(iv) above) below were used with NOESY or ROESY spectra recorded at a single mixing time (300 or 400 ms). In B, the cross peaks were subdivided into four ‘bins’ from ‘strong’ (s), ‘medium’ (m), ‘weak’ (w), ‘very weak’ (vw), based on the relative peak heights. Strong cross peaks were those with intensity $I > (1/2)I_{\text{MAX}}$, where I_{MAX} corresponds to the most intense cross peak in the spectrum; medium peaks had intensities I_{M} in the range $(1/4)I_{\text{MAX}}$ to $(1/2)I_{\text{MAX}}$, weak from $(1/8)I_{\text{MAX}}$ to $(1/4)I_{\text{MAX}}$, etc. Each bin was assigned a corresponding maximum constraint distance of 2.7 Å for s, 3.0 Å for m, 3.3 Å for w, 3.6 Å for vw, these ranges corresponding to approximately one standard deviation greater distance than the average found experimentally for each bin. The simplest approach (type (iii) and (iv) above) used a constraint distance of 2.7 or 3.3 Å, respectively, for any detectable NOE, and was used for testing the method with data from the literature in which NOEs were indicated but no strength or distance estimate was given (e.g. **6** and **7**).^{7,8}

3.2. Molecular modeling

Molecular modeling using the ConGen routines¹⁴ was performed using SYBYL software (Version 6.3, Tripos, Inc. St Louis, MO) running on a Silicon Graphics Octane system having two R10000 250 MHz CPUs, part of the Canadian Bioinformatics Resource Network. The Tripos force field²² without the electrostatic term was used in molecular dynamics and in minimizations. Constraints were applied as an energy term to the force field:

$$E_i = \frac{1}{2}k(d_i - D_i)^2; \quad d_i > D_i, \quad E_i = 0; \quad d_i \leq D_i$$

Modeling with the HyperChem software and XMConGen routines was also performed with the above computer system and also with a Silicon Graphics Indigo II, using the MM2 force field. The HyperChem software did not allow constraints as above without major modification, so the energy term was instead applied in the form:

$$E_i = \frac{1}{2}k(d_i - D_i)^2 \quad \text{for all } d_i$$

where d_i is the interproton distance in the given model structure, and k is a variable force constant.

The procedures used were largely similar to those described previously¹⁴ i.e. a structure having the correct atomic connectivity but randomly inverted chiral centres was minimized first without constraints, and then with the constraints applied in full ($k=200\text{--}400 \text{ kcal mol}^{-1} \text{ \AA}^{-1}$). This was followed by a plateau period (200 fs) of dynamics at high temperature (6000–10,000 K, usually 8000 K) with the constraints applied, and an annealing period of 500–800 fs during which the temperature was lowered uniformly to 300 K. The constraints were removed at this point by setting the force constants to zero, and the unconstrained structure was minimized, stored in a database, and used as the starting point for the next cycle. The published version of ConGen¹⁴ allowed for user-imposed inversion of selected single or multiple sites in cases where high-temperature dynamics

fail to invert some chiral centres, but these were found unnecessary in current applications to spiroptides owing to the use of higher dynamics temperatures and faster computers. The results for each trial structure were obtained as a table showing the N interproton distances d_i corresponding to the constraints, the chirality in order of ascending carbon number, the energy, the number V of constraints that are violated by more than a set percentage (normally 10–20%), and the RMS deviation σ in Å, defined as $\sigma^2 = (1/N) \sum \sigma_i^2$, where $\sigma_i^2 = (d_i - D_i)^2$ if $d_i > D_i$; or $\sigma_i = 0$ when $d_i \leq D_i$. Typically runs consisted of 100–1000 cycles, and all constraints used force constants of 200–400 kcal mol⁻¹ Å⁻¹.

Acknowledgements

We thank Peter Spierenburg, James Sedgwick and Peter Lichodziejewski for programming the ConGen routines; Allan Cembella and Nancy Lewis for plankton biomass and cultured material; Patricia LeBlanc for isolation of compounds, Jeffrey Quilliam for trial applications of the software, and the Canadian Bioinformatics Resource for computer access. Issued as NRCC publication number 42344.

References

- Hu, T.; Curtis, J. M.; Walter, J. A.; Wright, J. L. C. *J. Chem. Soc., Chem. Commun.* **1995**, 2159–2161.
- Hu, T.; Curtis, J. M.; Walter, J. A.; Wright, J. L. C. *Tetrahedron Lett.* **1996**, *37*, 7671–7674.
- Hu, T.; Burton, I. W.; Cembella, A.; Curtis, J. M.; Quilliam, M. A.; Walter, J. A.; Wright, J. L. C. *J. Nat. Prod.* **2001**, *64*, 308–312.
- Yasumoto, T.; Oshima, Y.; Yamaguchi, M. *Bull. Jpn. Soc. Sci. Fish.* **1978**, *44*, 1249–1255.
- Cembella, A. D.; Lewis, N. I.; Quilliam, M. A. *Phycologia* **2000**, *39*, 67–74.
- Uemura, D.; Chou, T.; Haino, T.; Nagatsu, A.; Fukuzawa, S.; Zheng, S.; Chen, H. *J. Am. Chem. Soc.* **1995**, *117*, 1155–1156.
- Chou, D.; Kamo, O.; Uemura, D. *Tetrahedron Lett.* **1996**, *37*, 4023–4026.
- Chou, D.; Haino, T.; Kuramoto, M.; Uemura, D. *Tetrahedron Lett.* **1996**, *37*, 4027–4030.
- Takada, N.; Umemura, N.; Suenaga, K.; Chou, T.; Nagatsu, A.; Takeharu, H.; Yamada, K.; Uemura, D. *Tetrahedron Lett.* **2001**, *42*, 3491–3494.
- Takada, N.; Umemura, N.; Suenaga, K.; Uemura, D. *Tetrahedron Lett.* **2001**, *42*, 3495–3497.
- Seki, T.; Satake, M.; Mackenzie, L.; Kaspar, H. F.; Yasumoto, T. *Tetrahedron Lett.* **1995**, *36*, 7093–7096.
- Stewart, M.; Blunt, J. W.; Munro, M. H. G.; Robinson, W. T.; Hannah, D. J. *Tetrahedron Lett.* **1997**, *38*, 4889–4890.
- Miles, C. O.; Wilkins, A. L.; Stirling, D. J.; MacKenzie, A. L. *J. Agric. Food Chem.* **2000**, *48*, 1373–1376.
- Falk, M.; Spierenburg, P. F.; Walter, J. A. *J. Comp. Chem.* **1996**, *17*, 409–417.
- Reggelin, M.; Hoffmann, H.; Köch, M.; Mierke, D. F. *J. Am. Chem. Soc.* **1992**, *114*, 3272–3277.
- Reggelin, M.; Köch, M.; Conde-Frieboes, K.; Mierke, D. F. *Angew. Chem., Int. Ed. Engl.* **1994**, *33*, 753–755.
- Köch, M.; Junker, J. *J. Mol. Model.* **1997**, *3*, 403–407.
- Köch, M.; Junker, J. *J. Org. Chem.* **1997**, *62*, 8614–8615.
- Baleja, J. D.; Moul, J.; Sykes, B. D. *J. Magn. Reson.* **1990**, *87*, 375–384.
- McCauley, J. A.; Nagasawa, K.; Lander, P.; Mischke, S. G.; Semones, M. A.; Kishi, Y. *J. Am. Chem. Soc.* **1998**, *120*, 7647–7648.
- Haasnoot, C. A. G.; De Leeuw, F. A. A. M.; Altona, C. *Tetrahedron* **1980**, *36*, 2783–2792.
- Clark, M.; Cramer, R. D.; Van Opdenbosch, N. *J. Comp. Chem.* **1989**, *10*, 982–1012.